Genome-wide circadian rhythm detection methods: systematic evaluations and practical guidelines

Wenwen Mei[1,*], Zhiwen Jiang[1,*], Yang Chen[2], Li Chen[3], Aziz Sancar[4,5,#], Yuchao Jiang[1,5,6,#]

[1] Department of Biostatistics, Gillings School of Global Public Health, University of North Carolina, Chapel Hill, NC 27599, USA.

[2] Department of Statistics and Michigan Institute for Data Science, University of Michigan, Ann Arbor, MI 48109, USA.

[3] Department of Medicine and Center for Computational Biology and Bioinformatics, Indiana University School of Medicine, Indianapolis, IN 46202, USA.

[4] Department of Biochemistry and Biophysics, School of Medicine, University of North Carolina, Chapel Hill, NC 27599, USA.

[5] Lineberger Comprehensive Cancer Center, University of North Carolina, Chapel Hill, NC 27599, USA.

[6] Department of Genetics, School of Medicine, University of North Carolina, Chapel Hill, NC 27599, USA.

∗ These authors contributed equally.

To whom correspondence should be addressed. Email: aziz_sancar@med.unc.edu; yuchaoj@email.unc.edu.

ABSTRACT

Circadian rhythms are oscillations of behavior, physiology, and metabolism in many organisms. Recent advancements in omics technology make it possible for genome-wide profiling of circadian rhythms. Here, we conducted a comprehensive analysis of seven existing algorithms commonly used for circadian rhythm detection. Using gold-standard circadian and non-circadian genes, we systematically evaluated the accuracy and reproducibility of the algorithms on empirical datasets generated from various omics platforms under different experimental designs. We also carried out extensive simulation studies to test each algorithm's robustness to key variables, including sampling patterns, replicates, waveforms, signal-to-noise ratios, uneven samplings, and missing values. Furthermore, we examined the distributions of the nominal p-values under the null and raised issues with multiple testing corrections using traditional approaches. With our assessment, we provide method selection guidelines for circadian rhythm detection, which are applicable to different types of high-throughput omics data.

BACKGROUND

Circadian rhythms are approximately 24-hour oscillations of behavior, physiology, and metabolism that exist in almost all living organisms ranging from prokaryotes to mammals [1, 2]. Circadian rhythm is regulated by the circadian system, which consists of many "clock-controlled genes" that exhibit oscillatory patterns [1]. These oscillations provide organisms with an adaptive advantage by enabling them to predict and adjust to the variations within their environments [3]. Additionally, and perhaps more importantly, disruptions of circadian rhythms have shown to contribute to numerous diseases, including metabolic disorders, heart disease, and aging [4-7]. It is, therefore, of great importance and interest to perform genome-scale analysis of biological rhythms.

Recent advances in omics technologies, including both microarrays and next-generation sequencing, offer appealing platforms to identify circadian genes on a genome-wide scale. These have, indeed, led to the proposal of multifarious methodologies adopted from various fields including mathematics, statistics, astrophysics, etc. The earliest of the selected methods is Lomb-Scargle (LS) periodogram [8], an algorithm adapted from astrophysics that detects oscillations by comparing the data to sinusoidal reference curves of varying periods and phases [9, 10]. ARSER is an algorithm that employs autoregressive spectral estimation to predict periodicity and applies a harmonic regression model to fit the time-series [11]. Unlike the model-based LS and ARSER, JTK_CYCLE is a non-parametric method that detects oscillations by comparing the ranks of the measured values to a set of prespecified symmetric reference curves [3]. Both RAIN and eJTK_CYCLE build on the strengths of JTK_CYCLE: RAIN includes an additional set of asymmetric waveforms and examines the increasing and decreasing portions of the curve separately [12]; eJTK_CYCLE improves JTK_CYCLE by explicitly calculating the null distribution such that it accounts for multiple hypothesis testing and by including non-sinusoidal reference waveforms [13]. Based on the successes of the aforementioned methods, MetaCycle proposes an ensemble framework that integrates results from three different algorithms, LS, ARSER, and JTK_CYCLE [14]. The most recent method, BIO_CYCLE, is a deep neural network trained on both simulated and empirical circadian and noncircadian time-series [15]. More general information and characteristics of each method are summarized in Table 1.

Multiple studies [10, 16, 17] have evaluated the performance of different methods for circadian rhythm detection, showing discrepancies among the methods, whose performances depend on multiple factors including experimental designs, waveforms of interest, etc. However, there has not been, to our best knowledge, a comprehensive summary and evaluation of all existing methods to date. Here, we systematically assess the performance of the seven aforementioned algorithms for circadian rhythm detection: LS, ARSER, JTK_CYCLE, RAIN, eJTK_CYCLE, MetaCycle, and BIO_CYCLE.

Specifically, we demonstrated and benchmarked the algorithms using real datasets with gold-standard circadian and non-circadian genes. All data were generated using the liver tissue from *Mus musculus* that had undergone two different experimental designs. Under the dark-dark experimental design (24-hour darkness), we focused on using data from gene expression microarrays to assess the accuracy and reproducibility of each algorithm; under the light-dark experimental design (12-hour light followed by 12-hour darkness), we adopted four different next-generation sequencing platforms and explored the robustness of each method in identifying circadian genes. In addition, we carried out extensive simulation studies to study how key variables, including sampling patterns, replicates, waveforms, signal-to-noise ratios, uneven samplings, missing values, affect the performance of each method. Lastly, we point out the flaw with using the Benjamini-Hochberg procedure to control for false discovery rate. Through these, we offer guidelines on experimental designs as well as best practices and methods of choice to increase the rigor and reproducibility in the analysis of large-scale circadian rhythms. To assist with the comparison of future methods and datasets using our framework, we provide detailed vignettes on applications of existing methods and performance evaluations with source code available at https://github.com/wenwenm183/Circadian_Genes_Benchmark.

RESULTS

Performance assessment using empirical datasets with dark-dark design

We first adopted three gene expression microarray datasets from Hughes et al. [18], Hughes et al. [19], and Zhang et al. [20]. For all three studies, mouse liver samples were collected in every hour or every two-hour under the dark-dark experimental design for 48

hours. We named these three datasets after the first author's last name and the year of publication as Hughes 2009, Hughes 2012, and Zhang 2014, respectively. In addition, we generated a new down-sampled dataset from the Hughes 2009 dataset by keeping the even time-points only, and named it “Down-sampled Hughes 2009”. Refer to Table 2A for details of the data. Figure 1 shows the scaled gene expression levels of four known circadian and four non-circadian genes. The circadian genes, including the well-studied *Clock*, *Cry1*, *Npas2*, and *Per1* [10], show oscillatory patterns that can be well reproduced across studies, while the non-circadian genes exhibit only noisy signals.

We set out to apply the seven algorithms to these four datasets to detect significantly cyclic genes and evaluate their performances using 104 circadian [10] and 113 non-circadian genes [21] from previous studies (Supplementary Table 1). The accuracy of each method in Hughes 2009, Down-sampled Hughes 2009, Hughes 2012, and Zhang 2014 was first assayed with the precision and recall rates for each algorithm given three p-value thresholds, 0.000005 (Bonferroni), 0.00005, 0.0005, and one q-value threshold 0.05 (Benjamini-Hochberg). Due to the tradeoff between sensitivity and specificity, with more relaxed thresholds of significance, the precision rates of all methods decrease while the recall rates increase – the 0.05 q-value threshold achieves the lowest precision rate yet the highest recall rate for any given method (Figure 2A). While there does not exist a single method that consistently achieves the highest precision or recall rate, JTK_CYCLE and BIO_CYCLE are more effective in controlling for false positives while still detecting true circadian genes. For the other methods, however, there is a much higher variability in precision, especially in the Zhang 2014 dataset (Figure 2A). RAIN and MetaCycle tend to have the highest sensitivity/recall, but this can come with significant sacrifice on precision (Figure 2A).

In addition, we find that higher sampling frequency can significantly improve the recall rates of all methods. While MetaCycle and RAIN achieve the apparently higher recall rate under different thresholds in dataset sampled at a lower frequency (2 h/2 days), all methods, except for LS, produce comparable recall rates when applied to the Hughes 2009 dataset, which is sampled at 1 h/2 days (Figure 2A). Notably, when analyzing the three datasets with lower sampling frequencies, LS failed under all circumstances with recall rates less than 0.1 (Figure 2A). This is due to the extreme p-value distribution of

the method with a spike at one, which we will discuss in more detail under “Correlated multiple testing and non-uniform distribution of p-values under the null”.

We further computed with the receiver operating characteristic (ROC) curves with a varying threshold on the nominal p-values returned by each method (Figure 2B). The area under the curve (AUC) values serve as a joint measure of sensitivity and specificity and are above 0.80 across all benchmark results, suggesting that all methods achieve good sensitivities while controlling for false positive rates. BIO_CYCLE, the deep-learning-based method, achieves the best performance with the highest AUC across all datasets (Figure 2B).

Reproducibility assessment using empirical datasets with dark-dark design

Reproducibility is one of the core principles for any bioinformatic tools and yet it remains a challenge in the field of circadian rhythm detection, which has not been fully explored. To evaluate the reproducibility of the methods, we first compared and contrasted the significantly cyclic genes returned by each method across the four datasets. To make the input dimensions compatible, we selected a total of 7,570 common genes that are shared across datasets and adopted a q-value threshold of 0.05 for significance. The Venn diagrams in Figure 3A show the overlapping relationships of the significant genes returned by each method. While the experimental designs are the same and the observed gene expression measurements are highly concordant (Figure 1), significant discrepancies of the calling results are observed. Of the seven benchmarked methods, ARSER resulted in 721 overlapping significant genes, which is the highest. This is followed by RAIN, eJTK_CYCLE, MetaCycle, BIO_CYCLE, JTK_CYCLE, and LS with 613, 528, 485, 296, 204, and 0 mutually identified positives, respectively. As mentioned previously, LS failed in detecting any significant oscillations for three out of the four datasets.

To further assess the reproducibility of the methods, we computed the Jaccard index and the Sorensen index to measure the similarities among the results from each method. Details of these metrics are included in the Materials and Methods section. As a result, RAIN achieves one of the highest Jaccard indices for any pair of comparisons and ARSER achieves the highest overall Sorensen index across all datasets (Figure 3B). On

139 the other hand, our results indicate that JTK_CYCLE, eJTK_CYLE, and BIO_CYCLE
140 produce the lowest similarity metrics across all comparisons (Figure 3B).
141
142 **Performance assessment using empirical datasets with light-dark design**
143 Next, we adopted four datasets that underwent light-dark experimental design using
144 different next-generation sequencing platforms (i.e., RNA-seq [22], Nascent-seq [22],
145 GRO-seq [23], and XR-seq [24]) and named each one after its sequencing protocol (Table
146 2B). The four datasets have much fewer numbers of time-points compared to the datasets
147 from the dark-dark design, yet three of the four datasets have technical replicates (Table
148 2B). More details of the data can be found in the Materials and Methods section. The
149 oscillatory patterns of known circadian genes are apparent and similar among the various
150 sequencing technologies (Figure 4A), indicating good data quality.
151 ARSER, despite its high reproducibility, cannot handle replicates, and previous
152 studies have shown that data should never be concatenated [17]. Therefore, we focused
153 on assessing the performance of the other six methods. We first examined the distribution
154 of the nominal p-values of the 104 gold-standard circadian genes returned by each
155 method, visualized as beehive plots in Figure 4B, where LS is significantly underpowered
156 in the detection of circadian genes compared to the other methods, given any of the
157 sequencing platforms. This result can be attributed to LS's inability to effectively detect
158 circadian rhythms in datasets with low sampling resolution, which is concordant with our
159 previous results. Similarly, RAIN is also underpowered, especially for sequencing
160 platforms of Nascent-seq, RNA-seq, and XR-seq, which are datasets consisting of
161 replicates. Finally, we observe that JTK_CYCLE, eJTK_CYCLE, MetaCycle, and
162 BIO_CYCLE can withstand the sparse sampling and result in overall good performance.
163 To further assess the performances of the methods, we examined the number of
164 significant genes identified by each method with a false discovery rate (FDR) of 0.05. Of
165 the 9,481 mutual genes in the four datasets, LS and RAIN did not identify any significant
166 genes in any of the datasets (Figure 4B). This result aligns with the results from the
167 previous analysis, where we observed LS and RAIN being underpowered. JTK_CYCLE
168 and MetaCycle detected a relatively small number of significant genes by RNA-seq and
169 XR-seq. eJTK_CYCLE identified 1,510 significant genes by RNA-seq, and BIO_CYCLE

170 identified 1,970 significant genes by XR-seq. When comparing across different
171 sequencing platforms, we observe that the number of detected significant genes from
172 RNA-seq and XR-seq data is much higher than that of the GRO-seq and Nascent-seq
173 data. This implicates a potential deficiency in detecting gene expression rhythmicity by
174 measuring nascent transcripts.

175 With the identified significant genes, we further carried out a gene set enrichment
176 analysis using the DAVID web server [25, 26] with the default options. Results from the
177 KEGG pathway enrichment analysis are shown in Supplementary Table 2. We find that
178 circadian rhythm is significantly enriched by various algorithms, which are marked with
179 asterisks in Figure 4B. Specifically, we find that of the four methods that were able to
180 identify statistically significant genes from RNA-seq data, all have enriched circadian
181 rhythm pathway. Circadian rhythm is also enriched in the three lists of genes that were
182 identified by eJTK_CYCLE as well as two of the three lists of genes identified by
183 BIO_CYCLE.

184

185 **Performance assessment using synthetic datasets**

186 To provide guidelines for method selection, we evaluated the performance of the seven
187 methods in detecting circadian rhythm by simulations with known ground truths.
188 Examples of waveforms generated for the simulated datasets are shown in
189 Supplementary Table 3. We generated six groups of simulated datasets to investigate
190 how key factors affect the performance, including sampling patterns, replicates,
191 waveforms, signal-to-noise ratios (SNRs), uneven samplings, and missing values.
192 Supplementary Table 4 outlines the six groups of simulations and we leave the detailed
193 setup in the Materials and Methods section. Within each simulation group, we repeated
194 each assessment with three different sampling frequencies to determine whether
195 increasing sampling frequency may have an effect on the aforementioned factors. The
196 three sampling frequencies include 4 h/1 day (six time-points), 3 h/1 day (eight time-
197 points), and 2 h/1 day (twelve time-points) and the results are shown in Figure 5A, 5B,
198 and 5C, respectively.

199 ***Sampling patterns***

200 To determine whether increasing the sampling frequency or lengthening the time-window
201 is more important for each method, we first evaluated the results under the sampling
202 pattern of 4 h/1 day versus 8 h/2 days, 3 h/1 day versus 6 h/2 days, and 2 h/1 day versus
203 4 h/2 days. We did not find strikingly different results within each pair of comparison,
204 indicating that when the total number of data points are fixed, having a denser sampling
205 density and enlarging the sampling time-window tend to have similar impact on
206 performance. However, when we increase the number of data points, the performances
207 of all methods are improved, which is concordant with existing studies [16, 17].
208 BIO_CYCLE generally outperforms the other methods, especially in datasets with lower
209 sampling frequency and shorter time-window, while JTK_CYCLE is the most sensitive to
210 fewer observations.

211 ***Replicates***

212 To investigate the trade-off between replicates and sampling frequency, we compared
213 the results of higher sampling frequency without replicates to those of lower sampling
214 frequency with replicates. We first compared the dataset sampled at 4 h /1 day X1 to the
215 dataset sampled at 8 h/1 day X2. LS, JTK_CYCLE, eJTK_CYCLE, and MetaCycle show
216 better performance with replicates, while BIO_CYCLE performs significantly better on
217 densely sampled datasets without replicates. RAIN does not show any apparent
218 preference. Similar results are seen when we applied the methods to the dataset at 3 h/1
219 day without replicates and the dataset at 6 h/1 day with replicates. As expected, further
220 increasing the sampling resolution offsets the existing preferences that the methods have
221 for inclusion of replicates or higher sampling density.

222 ***Waveforms***

223 Supplementary Table 3 outlines the different types of periodic waveforms that we
224 generated *in silico* in three broad categories: stationary, non-stationary, and asymmetric
225 ones. Through our simulations, we find that all of the algorithms perform the best in
226 detecting non-stationary waveforms. Additionally, all methods, with the exception of
227 eJTK_CYCLE, perform better on stationary waveforms, compared to asymmetric
228 waveforms. eJTK_CYCLE and RAIN are the top two methods for identifying asymmetric
229 waveforms, which are expected due to their design. This is followed by LS, BIO_CYCLE

230 and ARSER. JTK_CYCLE is ineffective in identifying asymmetric waveforms with any
231 sampling frequency and thus affects the performance of MetaCycle.

232 ***Signal-to-noise ratios (SNRs)***

233 To test the effects of different noise levels on method performance, we generated various
234 datasets with signal-to-noise ratios of 3, 2, 1, and 0.5. For all methods, our results suggest
235 that the larger the SNRs, the higher the accuracy, as expected. eJTK_CYCLE and
236 BIO_CYCLE are overall the most robust to noises regardless of sampling frequency,
237 while ARSER and JTK_CYCLE are the most sensitive with the poorest performance. LS,
238 RAIN, and MetaCycle suffer from instability when the noise levels are high, which,
239 interestingly, is also confounded with the sampling frequency in different directions.

240 ***Uneven samplings***

241 To understand how well the methods deal with uneven samplings, we focus on the results
242 of datasets with one or more uneven time-points. Our results suggest that BIO_CYCLE
243 continuously outperforms the other compatible methods. Under a sparse sampling design,
244 RAIN and LS/MetaCycle suffer significantly from an increasing number of uneven
245 samplings; a dense sampling design, on the other hand, rescues both methods.

246 ***Missing values***

247 We generated datasets that contain 1%, 5%, and 10% missing data, and benchmarked
248 the four methods that allow missing values. Our results show that JTK_CYCLE failed with
249 a high proportion of missing values under a low sampling frequency (4 h/1 day). The
250 performance of RAIN degrades with an increasing proportion of missing values, while the
251 performance of LS and MetaCycle are invariant. Note that BIO_CYCLE can be applied to
252 datasets with missing values only if there are replicates and the missingness only pertains
253 to part of the replicates. We therefore did not include it in the benchmark.

254 ***Computational efficiency***

255 Last but not least, we evaluated the computational efficiency across all benchmarked
256 methods. For dataset with low sampling resolution, the execution times among the
257 methods are approximately the same (Supplementary Table 5). However, when analyzing
258 data of larger sizes, RAIN requires significantly more time compared to the other methods.
259 The running time for LS, ARSER, and BIO_CYCLE does not change much with varying

sampling frequency. The running time for MetaCycle, which integrates results from LS, JTK_CYCLE, and ARSER, is calculated as the total running time of the three methods.

Correlated multiple testing and non-uniform distribution of p-values under the null

To detect circadian rhythm across thousands of genes, multiple hypothesis testing corrections are needed [27]. A common FDR threshold of 0.05 is recommended by most methods and adjusted p-values (q-values) are returned by all methods except for RAIN. In the previous sections, we adopted both Bonferroni and Benjamini-Hochberg procedures for corrections. Here, we more carefully examine such procedures and point out a potential drawback resulted from both correlated multiple testing and non-uniform distributions of the nominal p-values under the null. We started with the observed expression measurements from the Hughes 2009 dataset and generated a "null" dataset by randomly permuting the time labels for each gene (Figure 6A). Such permutations not only deplete each gene's rhythmic signals but also disrupts any gene-gene correlations as observed in the raw data, which are high between genes in the same pathways (Figure 6B). As such, all genes upon permutations are under the true null and additionally all gene-level testing is independent.

Figure 6C shows the distributions of nominal p-values for each method when applied to the dataset before and after permutation. The "U-shaped" histograms of the p-values for LS, JTK_CYCLE, MetaCycle, and RAIN using the original data indicate that there is dependence among the variables in the data. This violates the underlying assumption of uniformity and raises a red flag for using Bonferroni or FDR for error control [27]. A few methods have been developed for p-value adjustment when the tests are correlated [28-30] and such issue has been specifically pointed out by Hutchison and Dinner [31] for circadian rhythm detection.

We further applied the methods to the permuted data without gene-gene correlations. The hypothesis testing by LS, JTK_CYCLE, RAIN, and MetaCycle are still overly conservative, while the testing procedures for ARSER and BIO_CYCLE are biased with an overabundance of p-values around 0.3 and 0.1, respectively. eJTK_CYCLE empirically calculates the null distribution of the p-values via permutations and its enhanced version, booteJTK, speeds up this calculation by approximating the null

distribution of the Kendall's tau using a Gamma distribution [32]. This indeed leads to a p-value distribution closest to the null. However, neither eJTK_CYCLE nor booteJTK handles missing values or uneven samplings, as demonstrated previously. As a summary, there is still room for method development to yield p-values that better match the underlying assumption of a uniformly distributed p-values under the null.

DISCUSSION

Here, we propose a benchmark framework to systematically evaluate the performance of seven circadian rhythm detection methods, using high-throughput omics data. The empirical datasets that we adopted in this paper were from microarray [18-20] and RNA-seq [22] to measure gene expression, Nascent-seq [22] and GRO-seq [23] to measure nascent RNA, and XR-seq [24] to measure transcription-coupled repair. While these omics data were generated from different platforms, they focus on directly or indirectly profiling transcription. It has been well studied that biological rhythm goes beyond the transcriptomic transcript-level oscillations [33]. For example, post-translational protein acetylation has been linked to circadian rhythm via mass spectrometry [34, 35]. Moreover, it has been shown that a large number of metabolites and proteins exhibit circadian oscillations [36-38]. The methods and the evaluation procedures are not limited to transcriptomic studies, but can also be applied to acetylomic, metabolomic, and proteomic experiments.

Given the assessment results from both simulations and empirical dataset anaylsis, as well as literature review of the seven methods, we have summarized the strengths and weaknesses of each method in Table 3. In general, LS, RAIN and MetaCycle are more versatile in that they can be applied to datasets with replicates, uneven samplings, or missing values. eJTK_CYCLE and BIO_CYCLE generally outperform the other methods under most situations except for handling missing values. On the other hand, JTK is sensitive to high noise levels and low sampling resolutions, and LS cannot detect any significant genes when sampling resolution is lower than 2 h/2 days with an FDR threshold of 0.05. The best detection algorithm depends on experimental designs and characteristics of the input data. Therefore, we have created two decision trees, one for

low sampling resolution and the other for high sampling resolution, that outline the recommended method(s) under different scenarios (Supplementary Figure 1).

Recent advances of high-throughput technologies enable circadian rhythm detection on the genome-wide scale. As with all genomic data, the multi-time-point omics data for circadian rhythm detection bear both technical and biological variability, which can bias the analysis if not properly accounted. Data normalization and batch effect correction are crucial to remove technical biases and artifacts [39]. Cross-subject variability in rhythmic profiles, especially for human subjects, is a non-negligible source of genetic variation that needs to be adjusted [14]. This is especially important in the case-control setting where multiple subjects are involved. While we did not particularly focus on differential analysis since it is outside the scope of this paper, a few methods, including LimoRhyde [40] and DODR [12] have been made available for differential rhythmicity analysis under different conditions.

Increasingly more circadian omics data are being made available through existing studies and databases [33, 41]. We showed, from our empirical studies, that the rhythmic signals can be well recapitulated across different studies and/or different platforms (Figure 1, Figure 4A). Meta-analysis and multi-omics data integration remain an open-ended question in circadian rhythm detection [42]. In addition, transfer learning has been applied to multiple genomic research domains in genomics [43] – to borrow information and to transfer knowledge from existing data deposited in public repositories remain one of the future directions. Similarly, across different methods, an ensemble framework, as implemented by MetaCycle, can potentially boost performance. However, as we have pointed out earlier, the instability issue needs to be addressed, especially when multiple drastically distinct results are to be integrated.

To our best knowledge, all existing studies for circadian rhythm detection resort to bulk-tissue omics data, which characterize an averaged profile across different cell types in a tissue. The inherent heterogeneity can bias the analysis with reduced power and/or inflated FDR. With the decreasing cost and the increasing popularity of single-cell omics techniques, to profile circadian rhythmicity at the cellular level and to disentangle within tissue heterogeneity with regard to biological rhythm can be of great impact.

352

353 **MATERIALS AND METHODS**

354 **Empirical datasets**

355 Three datasets under the dark-dark experimental design including Hughes 2009 [18],
356 Hughes 2012 [19], and Zhang 2014 [20] were downloaded from GEO, and all used
357 microarrays to profile gene expressions (Table 2A). Additionally, we obtained four
358 datasets under the light-dark experimental design from the different sequencing platforms,
359 including Nascent-sequencing (Nascent-seq) [22], RNA-sequencing (RNA-seq) [22],
360 Global Run-On sequencing (GRO-seq) [23], and eXcision Repair-sequencing (XR-seq)
361 [24] (Table 2B). Nascent-seq sequence transcribed RNAs, obtained from the nuclei
362 without formation of the 3' end [44]. GRO-seq measures nascent RNAs by mapping,
363 characterizing, and evaluating transcriptionally engaged polymerase [45]. GRO-seq and
364 Nascent-seq differ from traditional RNA-seq, in which the reads map to predominantly
365 introns, while RNA-seq mainly assays exons [44]. XR-seq profiles DNA excision repair
366 on the genome-wide scale with single-nucleotide resolution [46]. Here, we focus on XR-
367 seq data from the transcribed strand only – it has been shown that the transcription-
368 coupled repair from the transcribed strand is positively correlated with expression [47].

369 For quality control, we removed genes that had constant gene expression
370 measurements in all datasets and further removed genes with more than half zero gene
371 expression values in the light-dark datasets. In cases where multiple probes got mapped
372 to the same RefSeq loci, we averaged the gene expression of the probes using the limma
373 package [48], available in Bioconductor. For data normalization, robust multi-array
374 average (RMA) [49] and genechip RMA (GC-RMA) [50] were used to normalize the array
375 data; transcript per million (TPM) and reads per kilobase per million reads (RPKM) [51]
376 were used to normalize the transcriptomic sequencing data. We scaled the normalized
377 data within each gene to make them compatible for visualization only, as shown in Figure
378 1 and Figure 4A.

379

380 **Evaluation metrics**

381 To evaluate the performance of the benchmarked methods, we adopted a list of 104
382 circadian [10] and 113 non-circadian genes [21] in mouse liver as positive and negative

383 controls, respectively. See Supplementary Table 1 for a full list of these gold-standard
384 genes. With these gold-standard genes, we calculated metrics including the precision and
385 recall rates given a p-value or q-value significance threshold (Figure 2A). We further
386 calculated the AUC values of the ROC curves, as joint measures of sensitivity and
387 specificity (Figure 2B).

388 To assess the reproducibility of each method, we compared the results from the
389 four dark-dark datasets by calculating the number of overlapping genes, as well as the
390 Jaccard and Sorensen index as metrics for similarity (Figure 3). Venn diagrams are used
391 to display the number of overlapping cycling genes identified across different datasets by
392 each method. The Jaccard index measures the pairwise similarities of the significant
393 genes detected between each pair of datasets. Let A_i and A_j be the set of significant
394 genes from dataset i and j. The Jaccard similarity index is defined as

395 $$J(A_i, A_j) = \frac{|A_i \cap A_j|}{|A_i \cup A_j|}.$$

396 The Sorensen Index is used to characterize similarity across all datasets [52]:

397 $$S(A_i, A_j, A_k, \dots) = \frac{T}{T-1}\left(\frac{\sum_{i<j}|A_i \cap A_j| - \sum_{i<j<k}|A_i \cap A_j \cap A_k| + \sum_{i<j<k<l}|A_i \cap A_j \cap A_k \cap A_l| - \cdots}{\sum_i |A_i|}\right)$$

398 where T is the number of sets compared. Larger number of overlapping genes and larger
399 Jaccard/Sorensen index values indicate higher reproducibility of the methods.
400

401 **Simulation setup**

402 Each simulated dataset consists of 6,000 circadian and 6,000 non-circadian gene profiles.
403 Stationary circadian profiles with a period of 24 hours are used in each simulation group,
404 as outlined below. Note that when running the methods, we set the period range from 20
405 to 28 h for all methods except for eJTK_CYCLE and JTK_CYCLE, which either has a
406 fixed period of 24 h or adjusts the period on the fly. The amplitude of the waveforms is
407 sampled from a uniform distribution between 1 and 6; the phase shift is sampled from a
408 uniform distribution between 0 and 24 h; and the noise term is sampled from a standard
409 normal distribution. Flat waveforms are used to generate non-circadian profiles in all
410 simulation groups except for testing against non-stationary waveforms where linear lines
411 are used.

We first aimed to investigate whether higher sampling frequency or longer sampling time-window is more beneficial for each method. In this simulation group, we generated two datasets with different sampling frequencies and sampling time-windows. With six time-points, we generated one dataset at 4 h/1 day and another at 8 h/2 days; with eight time-points, we generated one dataset at 3 h/1 day and another at 6 h/2 days; with 12 time-points, we generated one dataset at 2 h/1 day and another at 4 h/2 days.

Next, we assessed whether the inclusion of replicates can offset the effect of low sampling frequency in methods' ability of detecting oscillations. Replicates are defined as multiple measurements taken at the same time-point. Specifically, we generated two datasets consisting of the same number of observations, with or without replicates: one at 4 h/1 day X1 and the other at 8 h/1 day X2. The sampling design of the other two pairs of datasets are 3 h/1 day X1 v.s. 6 h/1 day X2, and 2 h/1 day X1 v.s. 4 h/1 day X2.

Since biological rhythms can take on various waveforms, we generated three types of waveforms via simulation: stationary, non-stationary, and asymmetric curves. Supplementary Table 3 includes models that we adopted *in silico* to generate the corresponding waveforms. Specifically, the stationary waveforms include cosine, cosine 2, and cosine peak curves; the non-stationary waveforms include cosine damp, trend exponential, and trend linear curves; the asymmetric subgroup consists of only the saw-tooth waveform. We assessed the performance of the methods in identifying each category of the circadian waveforms.

The next three groups of simulations aimed to determine which methods are more robust to different levels of signal-to-noise ratios, uneven samplings, and missing values. Specifically, we generated four datasets with SNRs of 0.5, 1, 2, and 3. Signal-to-noise ratio is defined by taking the ratio of the empirical variance of cosine function and the variance of the noise, the latter of which is fixed at one. Uneven samplings are defined as designs whose time-points are not equally spaced. To investigate the effect of uneven samplings on performance, we generated datasets with one, two, or four uneven samplings. With six time-points, datasets with four uneven samplings cannot be generated as it would only have two time-points. For missing data, we generated three levels of missing data (1%, 5%, and 10%) at three fixed, randomly selected time-points.

Lastly, we generated three datasets with sampling patterns of 1 h/2 days, 2 h/2 days, and 4 h/2 days to compute the execution times for each method. We seek to identify the differences in computational efficiency among the methods and to explore the effect of increasing sampling resolution on the execution time. Each dataset consists of a total of 6,000 genes. All execution times are reported by running on a Macbook Pro (15-inch, 2019) with 2.3 GHz 8-Core Intel Core i9 and 16 GB memory.

DATA AND SOFTWARE AVAILABILITY

MetaCycle is an open-source R package available at https://github.com/gangwug/MetaCycle and is also used for individual analysis for LS, JTK_CYCLE, and ARSER. RAIN is a Bioconductor R package available at https://bioconductor.org/packages/rain/. eJTK_CYCLE was downloaded from https://github.com/alanlhutchison/empirical-JTK_CYCLE-with-asymmetry. BIO_CYCLE was downloaded from http://circadiomics.igb.uci.edu/BIO_CYCLE. All empirical datasets were downloaded from the NCBI Gene Expression Omnibus (https://www.ncbi.nlm.nih.gov/geo/). The accession numbers for dark-dark datasets are GSE11923, GSE30411, and GSE54652, respectively. The accession numbers for light-dark datasets are GSE59486, GSE36872, GSE36871 and GSE109938, respectively.

ACKNOWLEDGEMENTS

This work was supported by NIH Grants R35 GM118102 (to A.S.), R01 ES027255 (to A.S.), P01 CA142538 (to Y.J.), UL1 TR002489 (to Y.J.), and a pilot award from the UNC Computational Medicine Program (to Y.J.). We thank the Sancar Lab members and Dr. John Hogenesch for helpful discussions and feedback.

REFERENCES

1. Li J, Grant GR, Hogenesch JB, Hughes ME: **Considerations for RNA-seq analysis of circadian rhythms.** *Methods Enzymol* 2015, **551:**349-367.

2. Panda S, Antoch MP, Miller BH, Su AI, Schook AB, Straume M, Schultz PG, Kay SA, Takahashi JS, Hogenesch JB: **Coordinated transcription of key pathways in the mouse by the circadian clock.** *Cell* 2002, **109:**307-320.

473 3. Hughes ME, Hogenesch JB, Kornacker K: **JTK_CYCLE: an efficient nonparametric**
474 **algorithm for detecting rhythmic components in genome-scale data sets.** *J Biol Rhythms*
475 2010, **25:**372-380.

476 4. Asher G, Sassone-Corsi P: **Time for food: the intimate interplay between nutrition,**
477 **metabolism, and the circadian clock.** *Cell* 2015, **161:**84-92.

478 5. Partch CL, Green CB, Takahashi JS: **Molecular architecture of the mammalian circadian**
479 **clock.** *Trends Cell Biol* 2014, **24:**90-99.

480 6. Roenneberg T, Merrow M: **The Circadian Clock and Human Health.** *Curr Biol* 2016,
481 **26:**R432-443.

482 7. Levi F, Schibler U: **Circadian rhythms: mechanisms and therapeutic implications.** *Annu*
483 *Rev Pharmacol Toxicol* 2007, **47:**593-628.

484 8. Glynn EF, Chen J, Mushegian AR: **Detecting periodic patterns in unevenly spaced gene**
485 **expression time series using Lomb-Scargle periodograms.** *Bioinformatics* 2006, **22:**310-
486 316.

487 9. Wijnen H, Naef F, Young MW: **Molecular and statistical tools for circadian transcript**
488 **profiling.** *Methods Enzymol* 2005, **393:**341-365.

489 10. Wu G, Zhu J, Yu J, Zhou L, Huang JZ, Zhang Z: **Evaluation of five methods for genome-**
490 **wide circadian gene identification.** *J Biol Rhythms* 2014, **29:**231-242.

491 11. Yang R, Su Z: **Analyzing circadian expression data by harmonic regression based on**
492 **autoregressive spectral estimation.** *Bioinformatics* 2010, **26:**i168-174.

493 12. Thaben PF, Westermark PO: **Detecting rhythms in time series with RAIN.** *J Biol Rhythms*
494 2014, **29:**391-400.

495 13. Hutchison AL, Maienschein-Cline M, Chiang AH, Tabei SM, Gudjonson H, Bahroos N,
496 Allada R, Dinner AR: **Improved statistical methods enable greater sensitivity in rhythm**
497 **detection for genome-wide data.** *PLoS Comput Biol* 2015, **11:**e1004094.

498 14. Wu G, Anafi RC, Hughes ME, Kornacker K, Hogenesch JB: **MetaCycle: an integrated R**
499 **package to evaluate periodicity in large scale data.** *Bioinformatics* 2016, **32:**3351-3353.

500 15. Agostinelli F, Ceglia N, Shahbaba B, Sassone-Corsi P, Baldi P: **What time is it? Deep**
501 **learning approaches for circadian rhythms.** *Bioinformatics* 2016, **32:**i8-i17.

502 16. Deckard A, Anafi RC, Hogenesch JB, Haase SB, Harer J: **Design and analysis of large-scale**
503 **biological rhythm studies: a comparison of algorithms for detecting periodic signals in**
504 **biological data.** *Bioinformatics* 2013, **29:**3174-3180.

505 17. Hughes ME, Abruzzi KC, Allada R, Anafi R, Arpat AB, Asher G, Baldi P, de Bekker C, Bell-
506 Pedersen D, Blau J, et al: **Guidelines for Genome-Scale Analysis of Biological Rhythms.** *J*
507 *Biol Rhythms* 2017, **32:**380-393.

508 18. Hughes ME, DiTacchio L, Hayes KR, Vollmers C, Pulivarthy S, Baggs JE, Panda S, Hogenesch
509 JB: **Harmonics of circadian gene transcription in mammals.** *PLoS Genet* 2009, **5:**e1000442.

510 19. Hughes ME, Hong HK, Chong JL, Indacochea AA, Lee SS, Han M, Takahashi JS, Hogenesch
511 JB: **Brain-specific rescue of Clock reveals system-driven transcriptional rhythms in**
512 **peripheral tissue.** *PLoS Genet* 2012, **8:**e1002835.

513 20. Zhang R, Lahens NF, Ballance HI, Hughes ME, Hogenesch JB: **A circadian gene expression**
514 **atlas in mammals: implications for biology and medicine.** *Proc Natl Acad Sci U S A* 2014,
515 **111:**16219-16224.

516 21. Wu G, Zhu J, He F, Wang W, Hu S, Yu J: **Gene and genome parameters of mammalian**
517 **liver circadian genes (LCGs).** *PLoS One* 2012, **7:**e46961.

518 22. Menet JS, Rodriguez J, Abruzzi KC, Rosbash M: **Nascent-Seq reveals novel features of**
519 **mouse circadian transcriptional regulation.** *Elife* 2012, **1:**e00011.

520 23. Fang B, Everett LJ, Jager J, Briggs E, Armour SM, Feng D, Roy A, Gerhart-Hines Z, Sun Z,
521 Lazar MA: **Circadian enhancers coordinate multiple phases of rhythmic gene**
522 **transcription in vivo.** *Cell* 2014, **159:**1140-1152.

523 24. Yang Y, Adebali O, Wu G, Selby CP, Chiou YY, Rashid N, Hu J, Hogenesch JB, Sancar A:
524 **Cisplatin-DNA adduct repair of transcribed genes is controlled by two circadian**
525 **programs in mouse tissues.** *Proc Natl Acad Sci U S A* 2018, **115:**E4777-E4785.

526 25. Huang da W, Sherman BT, Lempicki RA: **Systematic and integrative analysis of large gene**
527 **lists using DAVID bioinformatics resources.** *Nat Protoc* 2009, **4:**44-57.

528 26. Huang da W, Sherman BT, Lempicki RA: **Bioinformatics enrichment tools: paths toward**
529 **the comprehensive functional analysis of large gene lists.** *Nucleic Acids Res* 2009, **37:**1-
530 13.

531 27. Storey JD, Tibshirani R: **Statistical significance for genomewide studies.** *Proc Natl Acad*
532 *Sci U S A* 2003, **100:**9440-9445.

533 28. Li J, Ji L: **Adjusting multiple testing in multilocus analyses using the eigenvalues of a**
534 **correlation matrix.** *Heredity (Edinb)* 2005, **95:**221-227.

535 29. Conneely KN, Boehnke M: **So many correlated tests, so little time! Rapid adjustment of**
536 **P values for multiple correlated tests.** *Am J Hum Genet* 2007, **81:**1158-1168.

537 30. Schwartzman A, Lin X: **The effect of correlation in false discovery rate estimation.**
538 *Biometrika* 2011, **98:**199-214.

539 31. Hutchison AL, Dinner AR: **Correcting for Dependent P-values in Rhythm Detection.**
540 *BioRxiv* 2017.

541 32. Hutchison AL, Allada R, Dinner AR: **Bootstrapping and Empirical Bayes Methods Improve**
542 **Rhythm Detection in Sparsely Sampled Data.** *J Biol Rhythms* 2018, **33:**339-349.

543 33. Ceglia N, Liu Y, Chen S, Agostinelli F, Eckel-Mahan K, Sassone-Corsi P, Baldi P: **CircadiOmics:**
544 **circadian omic web portal.** *Nucleic Acids Res* 2018, **46:**W157-W162.

545 34. Masri S, Patel VR, Eckel-Mahan KL, Peleg S, Forne I, Ladurner AG, Baldi P, Imhof A,
546 Sassone-Corsi P: **Circadian acetylome reveals regulation of mitochondrial metabolic**
547 **pathways.** *Proc Natl Acad Sci U S A* 2013, **110:**3339-3344.

548 35. Mauvoisin D, Atger F, Dayon L, Nunez Galindo A, Wang J, Martin E, Da Silva L, Montoliu I,
549 Collino S, Martin FP, et al: **Circadian and Feeding Rhythms Orchestrate the Diurnal Liver**
550 **Acetylome.** *Cell Rep* 2017, **20:**1729-1743.

551 36. Dallmann R, Viola AU, Tarokh L, Cajochen C, Brown SA: **The human circadian metabolome.**
552 *Proc Natl Acad Sci U S A* 2012, **109:**2625-2629.

553 37. Feng D, Lazar MA: **Clocks, metabolism, and the epigenome.** *Mol Cell* 2012, **47:**158-167.

554 38. Robles MS, Cox J, Mann M: **In-vivo quantitative proteomics reveals a key contribution**
555 **of post-transcriptional mechanisms to the circadian regulation of liver metabolism.**
556 *PLoS Genet* 2014, **10:**e1004047.

557 39. Jiang Y, Wang R, Urrutia E, Anastopoulos IN, Nathanson KL, Zhang NR: **CODEX2: full-**
558 **spectrum copy number variation detection by high-throughput DNA sequencing.**
559 *Genome Biol* 2018, **19:**202.

560 40. Singer JM, Fu DY, Hughey JJ: **Simphony: simulating large-scale, rhythmic data.** *PeerJ* 2019,
561 **7:**e6985.

562 41. Li X, Shi L, Zhang K, Wei W, Liu Q, Mao F, Li J, Cai W, Chen H, Teng H, et al: **CirGRDB: a**
563 **database for the genome-wide deciphering circadian genes and regulators.** *Nucleic Acids*
564 *Res* 2018, **46:**D64-D70.

565 42. Patel VR, Eckel-Mahan K, Sassone-Corsi P, Baldi P: **CircadiOmics: integrating circadian**
566 **genomics, transcriptomics, proteomics and metabolomics.** *Nat Methods* 2012, **9:**772-
567 773.

568 43. Eraslan G, Avsec Z, Gagneur J, Theis FJ: **Deep learning: new computational modelling**
569 **techniques for genomics.** *Nat Rev Genet* 2019, **20:**389-403.

570 44. Trott AJ, Menet JS: **Regulation of circadian clock transcriptional output by CLOCK:BMAL1.**
571 *PLoS Genet* 2018, **14:**e1007156.

572 45. Core LJ, Waterfall JJ, Lis JT: **Nascent RNA sequencing reveals widespread pausing and**
573 **divergent initiation at human promoters.** *Science* 2008, **322:**1845-1848.

574 46. Hu J, Adar S, Selby CP, Lieb JD, Sancar A: **Genome-wide analysis of human global and**
575 **transcription-coupled excision repair of UV damage at single-nucleotide resolution.**
576 *Genes Dev* 2015, **29:**948-960.

577 47. Yimit A, Adebali O, Sancar A, Jiang Y: **Differential damage and repair of DNA-adducts**
578 **induced by anti-cancer drug cisplatin across mouse organs.** *Nat Commun* 2019, **10:**309.

579 48. Ritchie ME, Phipson B, Wu D, Hu Y, Law CW, Shi W, Smyth GK: **limma powers differential**
580 **expression analyses for RNA-sequencing and microarray studies.** *Nucleic Acids Res* 2015,
581 **43:**e47.

582 49. Irizarry RA, Hobbs B, Collin F, Beazer-Barclay YD, Antonellis KJ, Scherf U, Speed TP:
583 **Exploration, normalization, and summaries of high density oligonucleotide array probe**
584 **level data.** *Biostatistics* 2003, **4:**249-264.

50. Wu Z, Irizarry RA, Gentleman R, Martinez-Murillo F, Spencer F: **A Model-Based Background Adjustment for Oligonucleotide Expression Arrays.** *Journal of the American Statistical Association* 2004, **99:**909-917.

51. Conesa A, Madrigal P, Tarazona S, Gomez-Cabrero D, Cervera A, McPherson A, Szczesniak MW, Gaffney DJ, Elo LL, Zhang X, Mortazavi A: **A survey of best practices for RNA-seq data analysis.** *Genome Biol* 2016, **17:**13.

52. Diserud OH, Odegaard F: **A multiple-site similarity measure.** *Biol Lett* 2007, **3:**20-22.

FIGURE & TABLE LEGENDS

Figure 1. Examples of circadian and non-circadian benchmark gene expressions among three datasets with dark-dark experimental design. Scaled gene expressions from selected (A) circadian genes including *Clock*, *Cry1*, *Npas2*, and *Per1* and (B) non-circadian genes including *Utp6*, *Mtf1*, *Cln3*, *Abcd4*.

Figure 2. Evaluation of seven methods by precision, recall rates and ROC curves. (A) A p-value threshold of 0.000005 (Bonferroni threshold), 0.00005, 0.0005, and a q-value threshold of 0.05 (FDR threshold) are adopted for each of the seven methods applied to the four dark-dark empirical datasets. A more relaxed threshold results in a higher recall rate, with FDR being the most sensitive, yet this also leads to a higher number of false positives with a lower precision rate. (B) ROC curves and AUC values using gold-standard circadian and non-circadian genes. Each method is evaluated across four dark-dark empirical datasets. Sensitivity and specificity are calculated using the nominal p-values by each method with varying threshold. BIO_CYCLE returns the highest AUC.

Figure 3. Evaluation of method reproducibility. (A) Venn diagrams display the number of cyclic genes that are significant by each method among the four dark-dark datasets. (B) Jaccard index and the Sorensen index are used as metrics for reproducibility for each method across the four datasets with the same experimental design.

Figure 4. Circadian rhythm detection under light-dark experimental design by GRO-seq, Nascent-seq, RNA-seq, and XR-seq. (A) Gene-specific measurements of nascent

617 RNA, RNA, and transcription-coupled repair of four circadian benchmark genes, *Clock*,
618 *Npas2*, *Cry1*, and *Per1* by four different sequencing platforms. The solid and dotted lines
619 are used for the first and second replicates respectively. (B) Beehive plots of negative log
620 p-values of circadian genes as positive controls. The number of significant genes
621 detected by each method with an FDR threshold of 0.05 are shown in parenthesis. The
622 asterisks denote significant GO enrichments of circadian rhythm pathway. The nominal
623 p-values by JTK_CYCLE, MetaCycle, and BIO_CYCLE are the most significant, while LS
624 and RAIN tend to be underpowered. ARS is not included in the analysis because it cannot
625 be applied to datasets with replicates.
626
627 **Figure 5. Performance assessment via simulation studies.** Seven circadian rhythm
628 detection methods are evaluated under different experimental designs to explore how
629 sampling patterns, replicates, waveforms, signal-to-noise ratios (SNRs), uneven
630 samplings, and missing values affect performance. Simulations under each design are
631 carried out with different sampling frequencies: (A) 4 h/1 day, (B) 3 h/1 day, and (C) 2 h/1
632 day. AUC values calculated from ground truths are used as metrics.
633
634 **Figure 6. Existing methods return non-uniformly distributed p-values under the null,**
635 **partially due to non-independent testing due to gene-gene correlations.** (A) Gene
636 expression values for the benchmark circadian gene *Cry1* before and after random
637 permutations of the time labels. (B) Heatmaps of pairwise correlation coefficients among
638 the top 200 highly variable genes from the Hughes 2009 dataset. The top illustrates the
639 gene-gene correlation coefficients calculated from raw data input, and the bottom shows
640 the gene-gene correlations after permutation. (C) The distributions of nominal p-values
641 for each method when applied to the dataset before and after permutation. Gene-gene
642 correlations, which are accounted for by eJTK_CYCLE, partially lead to the systematic
643 deviations from the null distributions. The hypothesis testing by LS, JTK_CYCLE, RAIN,
644 and MetaCycle are overly conservative, while ARSER's and BIO_CYCLE's testing
645 procedures are biased with an overabundance of p-values around 0.3 and 0.1,
646 respectively, under the null.
647

Table 1. Summary of seven existing methods for circadian rhythm detection. [a] BIO_CYCLE can be applied to datasets with missing values only if there are replicates and the missingness only pertains to part of the replicates.

Table 2. High-throughput mouse liver datasets adopted for circadian rhythm detection. (A) Dark-dark experimental design. (B) Light-dark experimental design.

Table 3. Pros and cons of circadian rhythm detection methods.

SUPPLEMENTARY FIGURE & TABLE LEGENDS

Supplementary Table 1. Circadian and non-circadian genes in *Mus muculus* liver as gold standard. The 104 circadian gene list is extracted from Supplementary Table 4 in Wu et al. [10] and the 113 non-circadian gene list is obtained from Supplementary Table 2 in Wu et al. [21].

Supplementary Table 2. Pathway enrichment analysis of significantly cyclic genes from the light-dark datasets. Functional annotations (KEGG pathway mapping) of the significant genes (q-values ≤ 0.05) are carried out using the the DAVID Bioinformatics Resources (https://david.ncifcrf.gov/). The list only contains significantly enriched pathways with a 0.05 cutoff of the p-values adjusted by Benjamini Hochberg.

Supplementary Table 3. *In silico* generated periodic v.s. non-periodic gene profiles. Three types of periodic waveforms are included: stationary, non-stationary, and asymmetric. The stationary and non-stationary subgroups consist of three forms of cosine curves. The asymmetric subgroup consists of a saw-tooth waveform. Flat or linear lines are adopted to generate non-periodic waveforms. The waveforms shown are constructed without noise. 'Amp', 'pha', and 'per' represent amplitude, phase and period, respectively.

Supplementary Table 4. Details of simulation setup and parameters used to *in silico* generate periodic and non-periodic profiles. Each simulation run consists of 6,000 periodic and 6,000 non-periodic gene profiles. All simulated waveforms have a period

length of 24, a phase shift that is uniformly distributed between 0 and 24, and a noise term with standard normal distribution. The amplitude is uniformly distributed between 1 and 6 for all groups except when testing for different signal-to-noise ratios (SNRs), which we define as the ratios of the empirical variances of the cosine function and the variances of the noise. Non-periodic profiles are sampled from a flat/linear function. “X 1” indicates no replicate and “X 2” indicates two replicates.

Supplementary Table 5. Evaluation of computational efficiency with different sampling rates. Each method is run on a dataset with a total of 6,000 genes. All programs are run on a Macbook Pro (15-inch, 2019) with 2.3 GHz 8-Core Intel Core i9 and 16 GB memory. Running time for MetaCycle is the sum of the runing time for LS, ARSER, and JTK_CYCLE. Running time for BIO_CYCLE does not include the time used to fit the deep neural network.

Supplementary Figure 1. Decision tree as user guidance on method selection. Both decision trees have decision rules for noise levels, uneven samplings, replicates, and missing values. (A) Method selection for data with low sampling resolution. (B) Method selection for data with high sampling resolution.

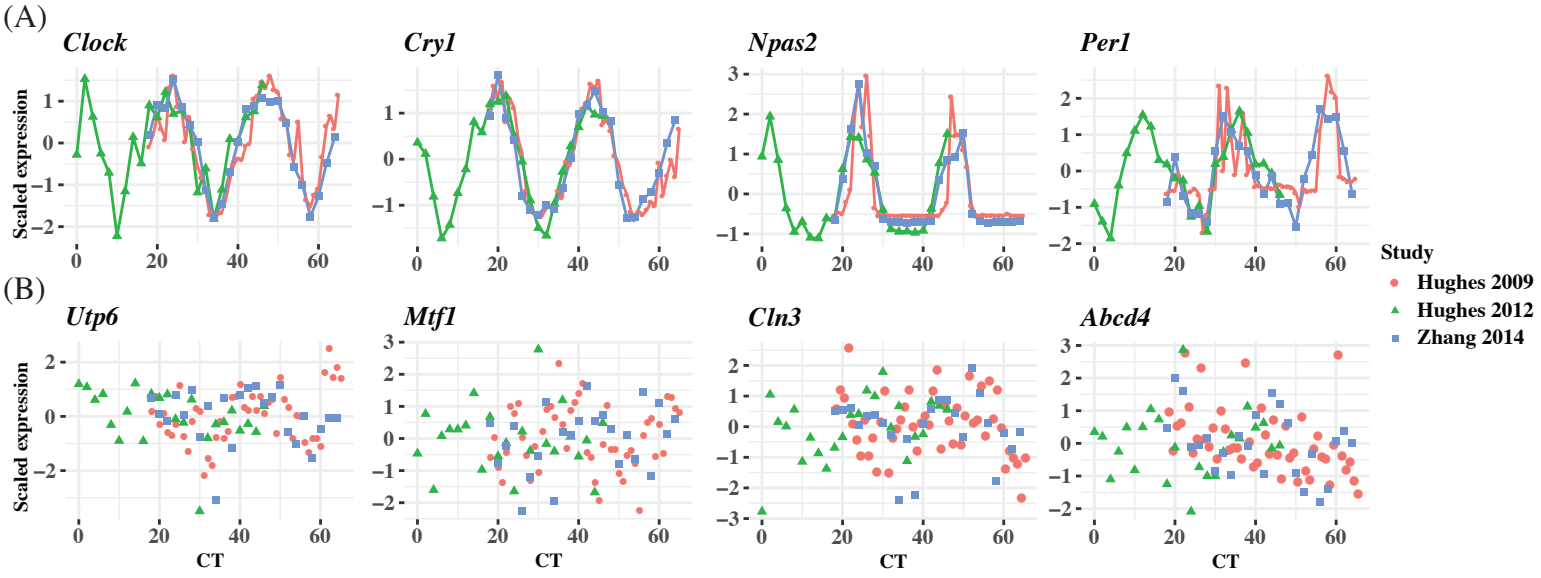
(A)
Clock
Cry1
Npas2
Per1
(B)
Utp6
Mtf1
Cln3
Abcd4
Scaled expression
CT
Study
Hughes 2009
Hughes 2012
Zhang 2014

Figure 1

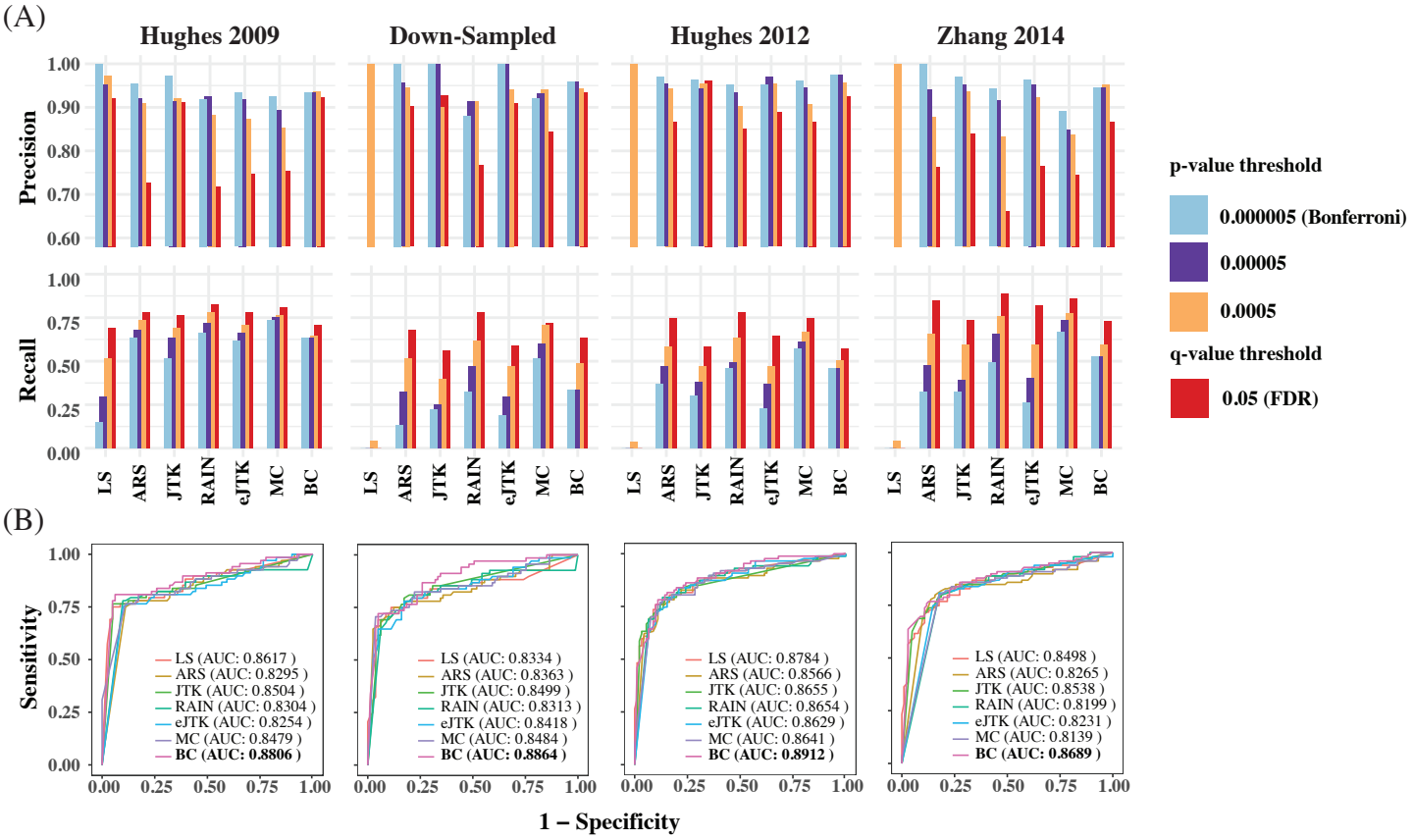
(A)
Hughes 2009
Down-Sampled
Hughes 2012
Zhang 2014
Precision
Recall
1.00
0.90
0.80
0.70
0.60
0.75
0.50
0.25
0.00
LS
ARS
JTK
RAIN
eJTK
MC
BC
p-value threshold
0.000005 (Bonferroni)
0.00005
0.0005
q-value threshold
0.05 (FDR)
(B)
Sensitivity
1 – Specificity
LS (AUC: 0.8617)
ARS (AUC: 0.8295)
JTK (AUC: 0.8504)
RAIN (AUC: 0.8304)
eJTK (AUC: 0.8254)
MC (AUC: 0.8479)
BC (AUC: 0.8806)
LS (AUC: 0.8334)
ARS (AUC: 0.8363)
JTK (AUC: 0.8499)
RAIN (AUC: 0.8313)
eJTK (AUC: 0.8418)
MC (AUC: 0.8484)
BC (AUC: 0.8864)
LS (AUC: 0.8784)
ARS (AUC: 0.8566)
JTK (AUC: 0.8655)
RAIN (AUC: 0.8654)
eJTK (AUC: 0.8629)
MC (AUC: 0.8641)
BC (AUC: 0.8912)
LS (AUC: 0.8498)
ARS (AUC: 0.8265)
JTK (AUC: 0.8538)
RAIN (AUC: 0.8199)
eJTK (AUC: 0.8231)
MC (AUC: 0.8139)
BC (AUC: 0.8689)

Figure 2

(A)

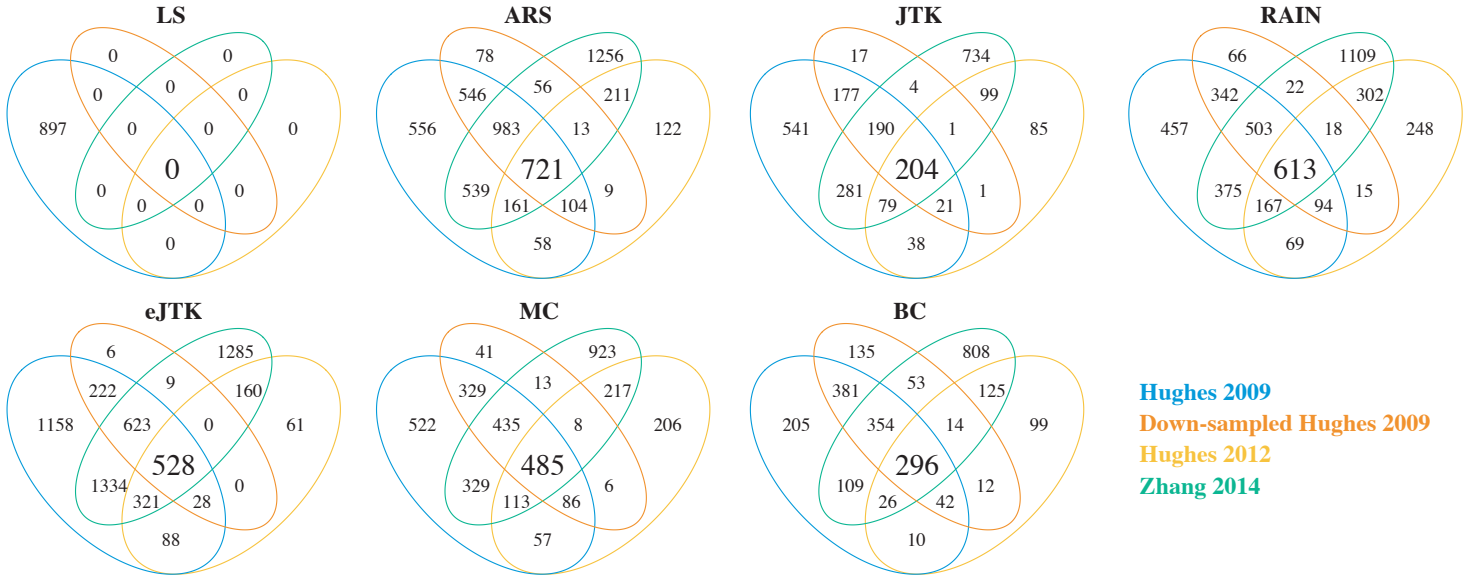

(B)

LS
Sorensen Index = 0

	Hughes 2009	Down-sample	Hughes 2012	Zhang 2014
Hughes 2009	0	0	0	
Down-sample		NA	NA	
Hughes 2012			NA	
Zhang 2014				

ARS
Sorensen Index = 0.7067

	Hughes 2009	Down-sample	Hughes 2012	Zhang 2014
Hughes 2009	0.6156	0.2595	0.4620	
Down-sample		0.2766	0.3791	
Hughes 2012			0.2613	
Zhang 2014				

JTK
Sorensen Index = 0.5607

	Hughes 2009	Down-sample	Hughes 2012	Zhang 2014
Hughes 2009	0.3810	0.1992	0.3183	
Down-sample		0.2478	0.2207	
Hughes 2012			0.2205	
Zhang 2014				

RAIN
Sorensen Index = 0.6762

	Hughes 2009	Down-sample	Hughes 2012	Zhang 2014
Hughes 2009	0.5662	0.2944	0.4073	
Down-sample		0.3009	0.3188	
Hughes 2012			0.3112	
Zhang 2014				

eJTK
Sorensen Index = 0.6379

	Hughes 2009	Down-sample	Hughes 2012	Zhang 2014
Hughes 2009	0.3245	0.2136	0.4875	
Down-sample		0.2717	0.2569	
Hughes 2012			0.2274	
Zhang 2014				

MC
Sorensen Index = 0.6595

	Hughes 2009	Down-sample	Hughes 2012	Zhang 2014
Hughes 2009	0.5507	0.2653	0.3873	
Down-sample		0.2931	0.3152	
Hughes 2012			0.2860	
Zhang 2014				

BC
Sorensen Index = 0.6381

	Hughes 2009	Down-sample	Hughes 2012	Zhang 2014
Hughes 2009	0.6555	0.2236	0.3240	
Down-sample		0.2353	0.3045	
Hughes 2012			0.2367	
Zhang 2014				

Figure 3

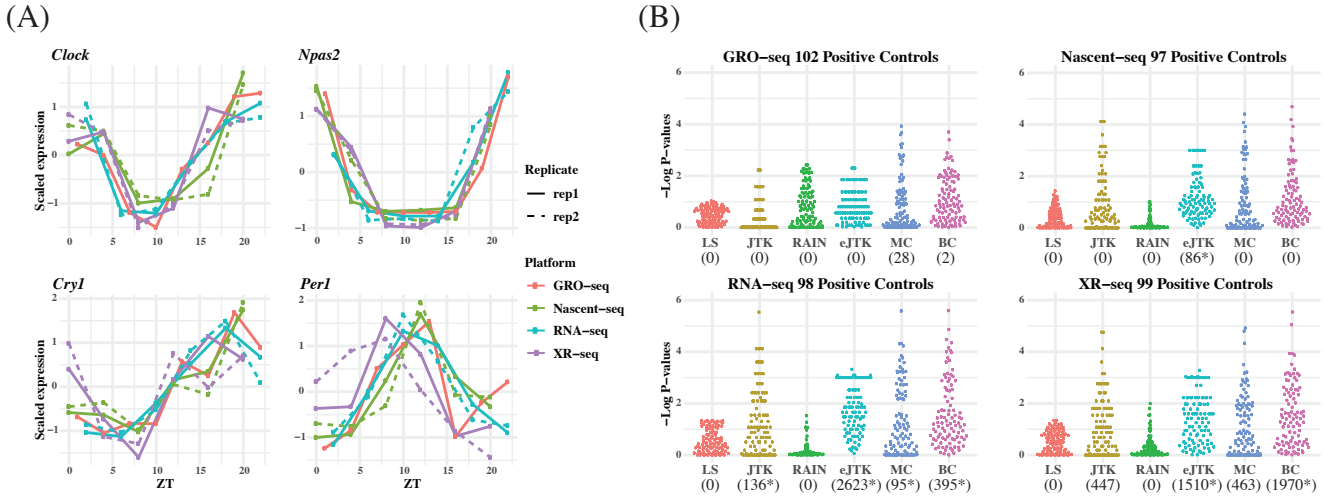
(A)
Clock
Npas2
Cry1
Per1
Scaled expression
ZT
Replicate
rep1
rep2
Platform
GRO−seq
Nascent−seq
RNA−seq
XR−seq
(B)
GRO−seq 102 Positive Controls
Nascent−seq 97 Positive Controls
RNA−seq 98 Positive Controls
XR−seq 99 Positive Controls
−Log P−values
LS (0)
JTK (0)
RAIN (0)
eJTK (0)
MC (28)
BC (2)
LS (0)
JTK (0)
RAIN (0)
eJTK (86*)
MC (0)
BC (0)
LS (0)
JTK (136*)
RAIN (0)
eJTK (2623*)
MC (95*)
BC (395*)
LS (0)
JTK (447)
RAIN (0)
eJTK (1510*)
MC (463)
BC (1970*)

Figure 4

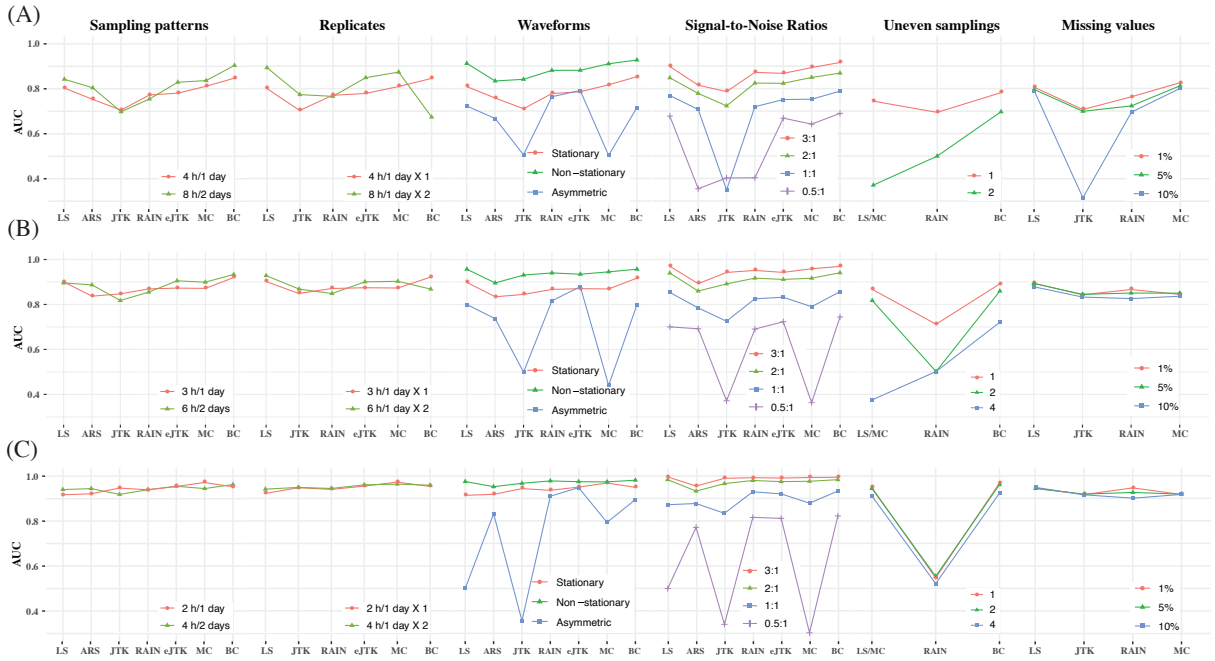
(A)
Sampling patterns
Replicates
Waveforms
Signal-to-Noise Ratios
Uneven samplings
Missing values
AUC
4 h/1 day
8 h/2 days
4 h/1 day X 1
8 h/1 day X 2
Stationary
Non−stationary
Asymmetric
3:1
2:1
1:1
0.5:1
1
2
1%
5%
10%
LS ARS JTK RAIN eJTK MC BC
LS JTK RAIN eJTK MC BC
LS/MC RAIN BC
LS JTK RAIN MC
(B)
3 h/1 day
6 h/2 days
3 h/1 day X 1
6 h/1 day X 2
4
(C)
2 h/1 day
4 h/2 days
2 h/1 day X 1
4 h/1 day X 2

Figure 5

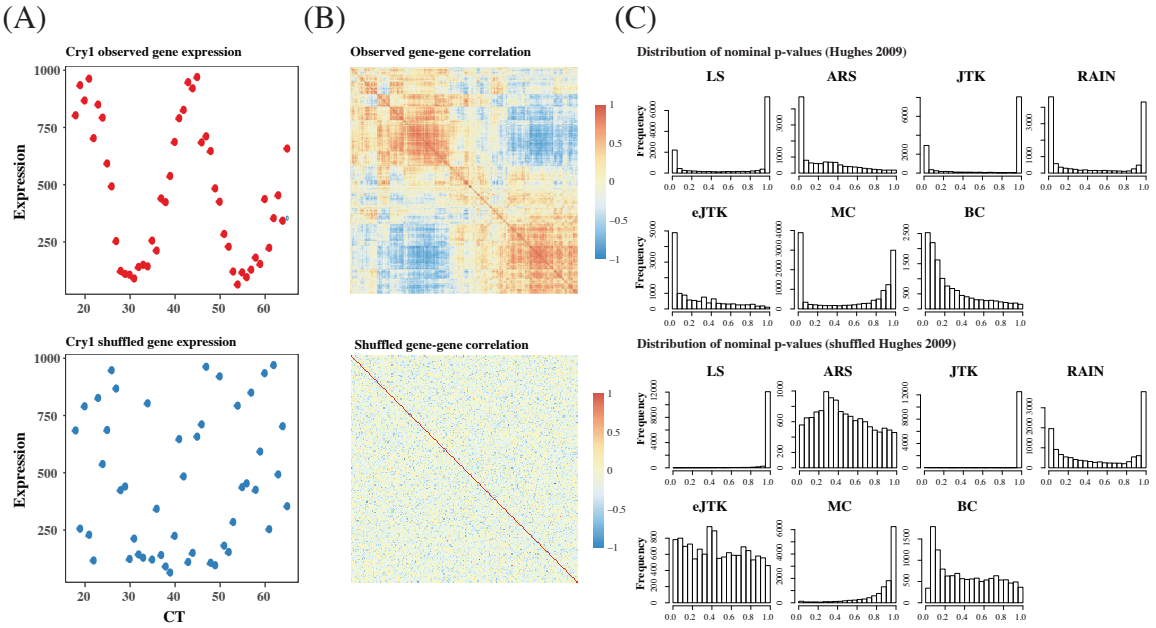
(A)
(B)
(C)
Cry1 observed gene expression
Expression
Observed gene-gene correlation
Distribution of nominal p-values (Hughes 2009)
LS
ARS
JTK
RAIN
eJTK
MC
BC
Frequency
Cry1 shuffled gene expression
CT
Shuffled gene-gene correlation
Distribution of nominal p-values (shuffled Hughes 2009)

Figure 6

Package	Method Key Words	Method Type	Reference	Availability	Language	Replicates	Missing Values	Uneven Sampling
Lomb-Scargle (LS)	Periodogram	Parametric	*Bioinformatics (2006)*	https://www.iiap.res.in/astrostat/tuts/Lomb-Scargle.html	R	✔	✔	✔
ARSER (ARS)	Harmonic Regression	Parametric	*Bioinformatics (2010)*	http://bioinformatics.cau.edu.cn/ARSER	Python & R	✕	✕	✕
JTK_CYCLE (JTK)	Kendall's Tau	Non-parametric	*J Biol Rhythms (2010)*	https://openwetware.org/wiki/HughesLab:JTK_Cycle	R	✔	✔	✕
RAIN	Asymmetric waveforms	Non-parametric	*J Biol Rhythms (2014)*	http://bioconductor.org/packages/rain	R	✔	✔	✔
eJTK_CYCLE (eJTK)	Empirical p-values	Non-parametric	*PLOS Comp. Bio. (2015)*	https://github.com/alanlhutchison/empirical-JTK_CYCLE-with-asymmetry	Python	✔	✕	✕
MetaCycle (MC)	Integration	Parametric	*Bioinformatics (2016)*	https://cran.r-project.org/package=MetaCycle	R	✔	✔	✔
BIO_CYCLE (BC)	Deep Neural Network	Parametric	*Bioinformatics (2016)*	http://circadiomics.igb.uci.edu	R	✔	✔/✕[a]	✔

Table 1

Design	Name	Reference	Accession Number	Tissue Type	Sequencing Platform	Number of Time Points & Replicates	Number of Genes	Time Points
(A) Dark-Dark	Hughes et al.	*PLOS Genetics (2009)*	GSE11923	Liver	Microarray	48 x 1	13,029	CT18, 19, 20, …, 65
	Hughes et al. (down-sampled)	*PLOS Genetics (2009)*	GSE11923	Liver	Microarray	24 x 1	12,506	CT18, 20, 22, …, 64
	Hughes et al.	*PLOS Genetics (2012)*	GSE30411	Liver	Microarray	24 x 1	14,413	CT0, 2, 4, …, 46
	Zhang et al.	*PNAS (2014)*	GSE54652	Liver	Microarray	24 x 1	20,307	CT18, 20, 22, …, 64
(B) Light-Dark	Fang et al.	*Cell (2014)*	GSE59486	Liver	GRO-seq	8 x 1	17,463	ZT1, 4, 7, 10, 13, 16, 19, 22
	Menet et al.	*eLIFE (2012)*	GSE36872	Liver	Nascent-seq	6 x 2	17,917	ZT0, 4, 8, 12, 16, 20
	Menet et al.	*eLIFE (2012)*	GSE36871	Liver	RNA-seq	6 x 2	17,222	ZT2, 6, 10, 14, 18, 22
	Yang et al.	*PNAS (2018)*	GSE109938	Liver	XR-seq (TS)	6 x 2	17,652	ZT0, 4, 8, 12, 16, 20

Table 2

Methods	Pros	Cons
LS	• Effective in handling missing values • Not restricted by input data structure (i.e. can be applied to datasets with replicates, uneven samplings, or missing values)	• Rapid degradation in detectability when applied to datasets with low sampling resolution • U-shaped *p*-values distribution • Sensitive to outliers
ARSER	• High reproducibility	• Cannot handle replicates, uneven samplings, or missing values
JTK_CYCLE	• High precision • Robust to outliers	• Incapable of detecting asymmetric waveforms • U-shaped *p*-values distribution • Sensitive to high level of noise • High false negative rates • Low reproducibility
RAIN	• High recall • Effective in detecting asymmetric waveforms • High reproducibility • Not restricted by input data structure	• High false positive rates • U-shaped *p*-values distribution • Computationally intensive with increasing sampling resolution
eJTK_CYCLE	• Uniform distribution of nominal *p*-values • Most effective in detecting asymmetric waveforms • Handle data with replicates, various signal-to-noise ratios, sampling patterns and waveforms effectively	• Unable to test different periods simultaneously • Cannot handle missing values or uneven samplings
MetaCycle	• High recall • Not restricted by input data structure • Offset the disadvantages of one method with the other two among LS, ARSER and JTK_CYCLE • Directly return calling results from three perspective methods and perform ensemble	• P-values generated with Fisher's integration require independence assumption • Integrated results can be biased by the poor performance of one method as the ensemble weights are the same for all methods
BIO_CYCLE	• Most effective in controlling for false positive rates • Most robust to data with high noise, uneven samplings, and low sampling resolutions • High precision • High computational efficiency with pre-trained model	• Require extensive time to train the DNN model • Handle missing values only if data have replicates and the missingness only pertains to part of the replicates • Low reproducibility

Table 3